

Chemical Modification of Oil Palm Empty Fruit Bunch: Determination of Optimum Condition and Characterization

G. S. Tay, H. D. Rozman

School of Industrial Technology, Universiti Sains Malaysia, 11800 Minden, Penang, Malaysia

Received 27 November 2005; accepted 22 April 2007

DOI 10.1002/app.26825

Published online 17 July 2007 in Wiley InterScience (www.interscience.wiley.com).

ABSTRACT: In this study, optimum condition for the reaction of glycidyl methacrylate (GMA), epichlorohydrin (ECH), and propylene oxide (PO) with oil palm empty fruit bunch (EFB) were determined. The treated EFB was characterized using Fourier transform infrared (FTIR), wide-angle X-ray diffraction (WAXD), and differential scanning calorimeter (DSC). It is evident from FTIR analysis that all the reagents used were chemically attached to the EFB. From the results of hydroxyl (OH) group determination, it was shown that for all types of reaction, except ECH reaction, more OH groups are generated and accessi-

ble. However, no significant difference is observed as the modification level was increased. The density of treated EFB regardless of the types of reaction was relatively lower than that of the untreated EFB. From WAXD analysis, it was found that the crystallinity of EFB was disrupted when the modification level achieved about 30%. © 2007 Wiley Periodicals, Inc. *J Appl Polym Sci* 106: 1697–1706, 2007

Key words: lignocellulosic; oil palm empty fruit bunch; chemical modification

INTRODUCTION

Recently, utilization of lignocellulosic materials in making composites has received considerable attention. This has been attributed to several advantages offered by lignocellulosic fillers, such as lower density, greater deformability, less abrasiveness to equipment, biodegradability, and lower cost. However, in making good-polymer composite, in term of mechanical and physical properties, the main obstacle to be resolved is the compatibility between the lignocellulosic material and the polymer matrix. Generally, there are two types of interaction at the interfacial region, i.e., covalent and hydrogen bondings, respectively. While, covalent bonding at the interfacial region exists in thermoplastic-wood composites with incorporation of a coupling agent, it is more prevalent in thermoset-lignocellulosic composites. This is because lignocellulosic hydroxyl (OH) groups could serve as reaction sites with various functional groups in the thermoset system.

There have been attempts to chemically modify lignocellulosic materials to improve the interfacial properties of a composite.^{1–3} According to Rowell,⁴ chemical modification of lignocellulosic materials or

wood was introduced primarily to enhance the resistance to degradation reaction, including biological, ultraviolet, and thermal degradation. This subsequently resulted in the improvement of mechanical strength and dimensional stability on the chemically modified lignocellulosic materials. In recent years, attention has shifted to the interfacial properties of lignocellulosic-based composite. Baiardo et al.¹ had prepared esterified and etherified steam exploded flax. They found that only small fraction of cellulose OH involved in these reactions. Mwaikambo and Ansell² had studied chemical modification on various types of lignocellulosic materials by alkalinization. From the results obtained, they concluded that the treated lignocellulosic materials showed enhanced fiber-resin adhesion. Santayanan and Wootthikanokkhan³ reported that the compatibility of cassava starch with PU matrix has been improved upon acylation.

This study was embarked to develop glycidyl methacrylate (GMA), epichlorohydrin (ECH) and propylene oxide (PO) modified oil palm empty fruit bunch (EFB). It is believed that by chemically modifying the lignocellulosic with appropriate reagents, more functional groups would be introduced and/or make more of these groups especially hydroxyl group accessible for reaction with PU system. This would in turn increase the stress transfer efficiency and be reflected in the physical and mechanical properties of the PU-lignocellulosic composites.

Correspondence to: G. S. Tay (tguanseng@gmail.com).

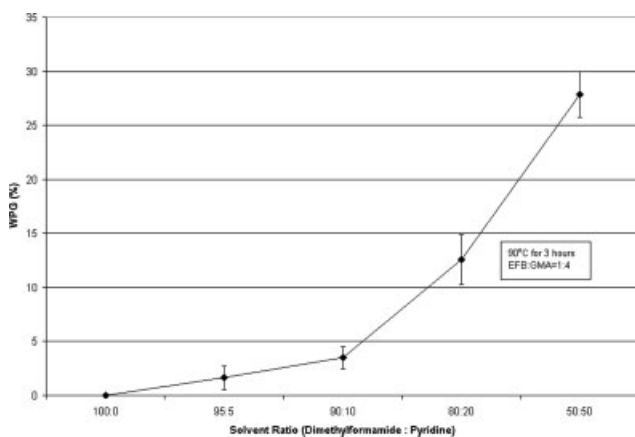


Figure 1 The effect of solvent ratio (DMF : pyridine) on GMA-modified EFB WPG (90°C, 3 h, EFB : GMA = 1 : 4).

METHODOLOGY

Materials

The EFB in the fiber form was obtained from Sabutek Sdn.Bhd., Teluk Intan, Perak, Malaysia. GMA and ECH were supplied by Fluka Chemika; PO and hydroquinone (Hq) were supplied by BDH Chemicals and Merck-Schuchardt, respectively.

Experimental

EFB particle preparation

The EFB fiber was washed under reflux condition with a solvent mixture (toluene : ethanol : acetone = 4 : 1 : 1 ratio, v/v) for 3 h to remove the impurities such as palm oil residues on the fiber surface before being ground. The EFB particle obtained was sieved to separate the particles with different sizes and only particles with mesh number 35–60 (0.500–0.250 mm) would be used in this study.

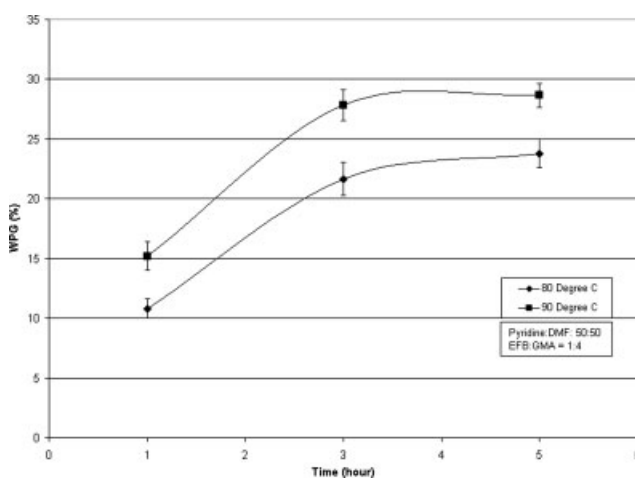


Figure 2 The effect of reaction temperature and reaction time on GMA-modified EFB WPG (EFB : GMA = 1 : 4).

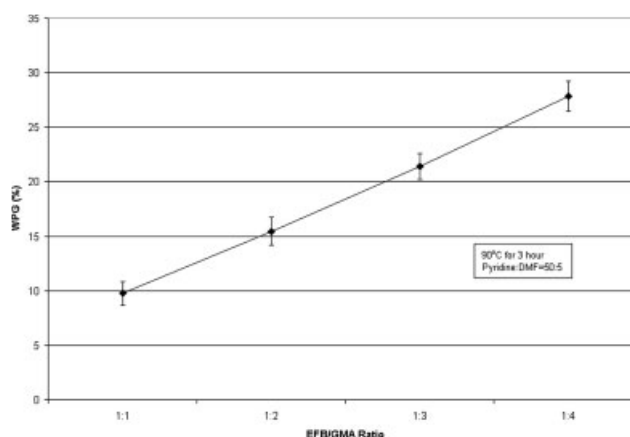


Figure 3 The effect of EFB : GMA ratio on GMA-modified EFB WPG (90°C, 3 h).

EFB modification with GMA

The oven-dried EFB was weighed and added into a 1-L round-bottomed reaction flask. The GMA/EFB = 4 : 1 (eq/eq) ratio was fixed constant, and the other parameters such as solvent mixture (DMF : pyridine), reaction time and temperature were varied to determine an optimum condition for reaction. The equivalent weight of EFB was determined by phthalation,⁵ which is 492. Small amount of Hq (5% based on GMA) was added to prevent homopolymerization from occurring between GMA.⁶ The round-bottomed flask was then placed in an oil bath to allow reaction to commence under a predetermined condition. The GMA-modified EFB produced was then washed with acetone under reflux condition for 2 h to remove the unreacted chemical reagents. The treated EFB was dried in a vacuum oven at 90°C before weight percentage gain (WPG) was determined. The WPG was calculated by the following equation:

$$\text{WPG (\%)} = \frac{W_m - W_d}{W_d} \times 100$$

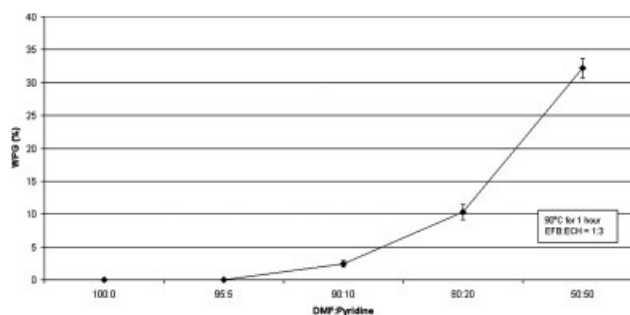


Figure 4 The effect of solvent ratio (DMF : pyridine) on ECH-modified EFB WPG (90°C, 1 h, EFB : ECH = 1 : 3).

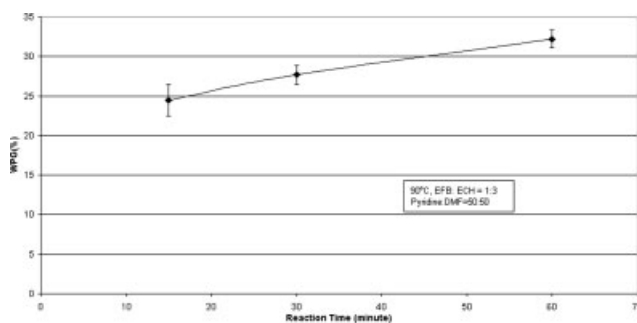


Figure 5 The effect of reaction time on ECH-modified EFB WPG (90°C, EFB : ECH = 1 : 3).

where W_m is the weight (g) of the oven-dried EFB after modification and W_d is the weight (g) of the oven-dried EFB before modification.

The obtained optimum condition was used to modify the EFB with different GMA/EFB ratios (1–4, eq/eq).

EFB modification with ECH

The procedure for preparation of ECH-modified EFB was similar to the aforementioned procedure except that the ratio of ECH/EFB was varied from 0.5 to 3 (eq/eq).

EFB modification with PO

The oven-dried EFB was weighed and added into a 1-L round-bottomed reaction flask. The PO/EFB = 6 : 1 (eq/eq) ratio was fixed constant, and the other parameters such as reaction time and temperature were varied to determine an optimum condition for reaction. In this modification, pyridine was used as a solvent as well as a swelling agent. A vigorous stream of nitrogen was applied for 1 min before starting the reaction. The reaction flask was placed in a water bath to allow reaction to take place under preset condition. The PO-modified EFB produced was then washed with acetone under reflux condition for 2 h to remove the unreacted chemical

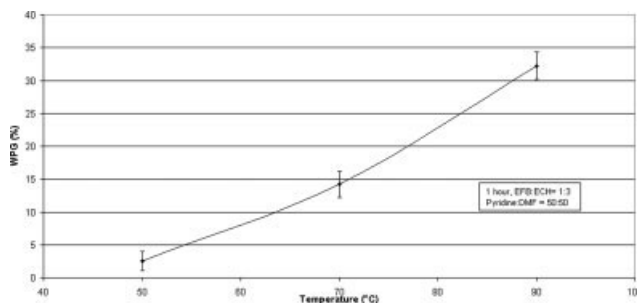


Figure 6 The effect of reaction temperature on ECH-modified EFB WPG (EFB : ECH = 1 : 3, 1 h).

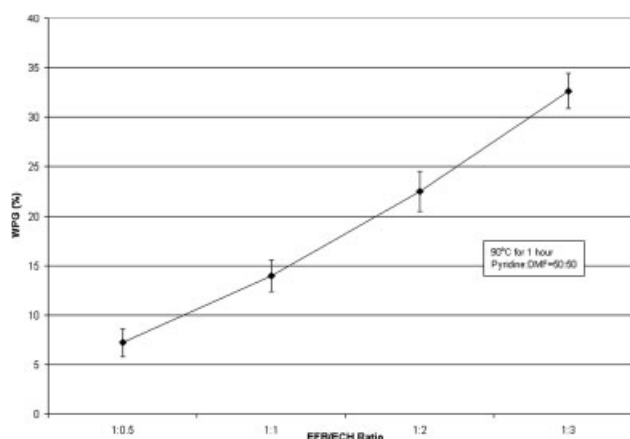


Figure 7 The effect of EFB : ECH ratio on ECH-modified EFB WPG.

reagents. The EFB was then oven-dried at 90°C before determining the WPG. The obtained optimum condition was used to modify the EFB with different PO content.

Characterization

Fourier transform infrared (FTIR)

The EFB (modified and unmodified) were ground into powder form, dried, and dispersed in dry potassium bromide (ratio of sample : KBr = 1 : 100). The mixture was then pressed into pellets. The samples were scanned using a Nicolet Avatar 360 FTIR in the range 4000–400 cm^{-1} , and 64 scans were done for each sample. The modified EFB sample obtained from optimum condition and highest WPG was used in this analysis.

Density determination

Pyrex[®] Gay-Lussac bottle [density bottle or specific gravity (SG) bottle] with capacity of 25 mL was used

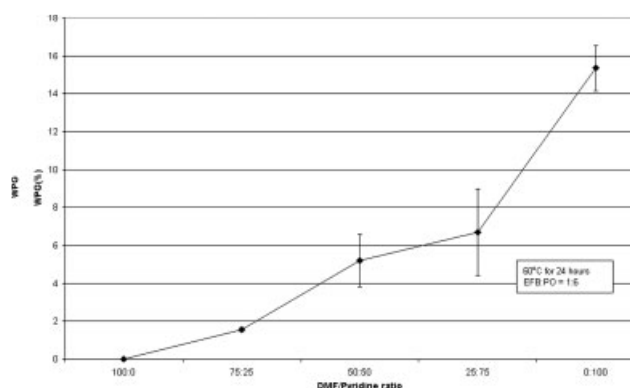


Figure 8 The effect of solvent ratio (DMF : pyridine) on PO-modified EFB WPG.

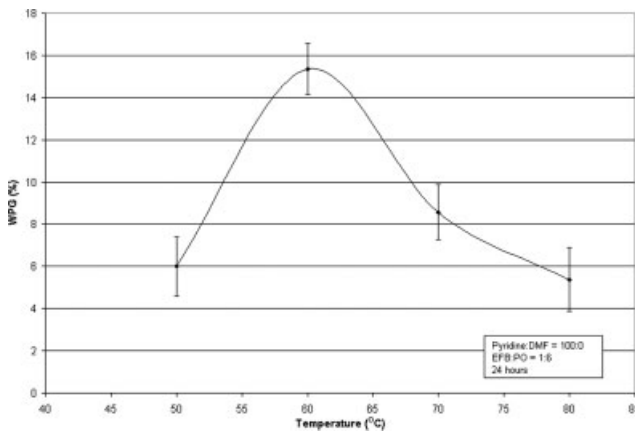


Figure 9 The effect of reaction temperature on PO-modified EFB WPG (24 h, EFB : PO = 1 : 6).

to determine the density of EFB (unmodified and modified). In this case, toluene was used, as the medium in measuring the density of the EFB because it is a nonswelling agent for most of the lignocellulosic materials. The equations shown below were used to calculate the density of EFB. The density of the composites was determined by measuring its dimensions and weight^{7,8}:

- Specific gravity of toluene, SG_T

$$SG_T = \frac{W_3 - W_1}{W_2 - W_1}$$

- Density of EFB, SG_{EFB}

$$SG_{EFB} = \frac{W_4 - W_1}{(W_3 - W_1) - (W_5 - W_4)} \times SG_T$$

where W_1 is the weight (g) of empty density bottle; W_2 , the weight (g) of density bottle filled with of dis-

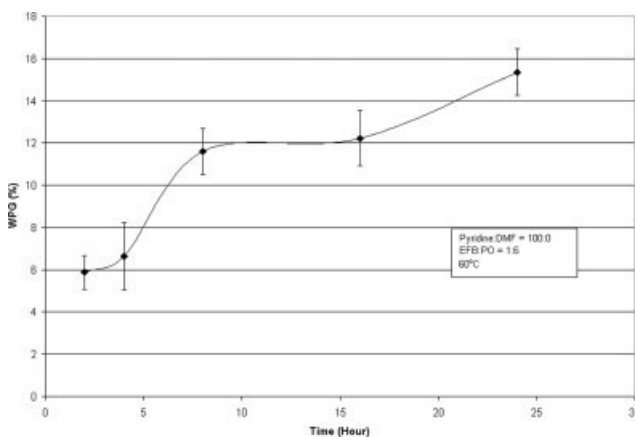


Figure 10 The effect of reaction time on PO-modified EFB WPG (60°C, EFB : PO = 1 : 6).

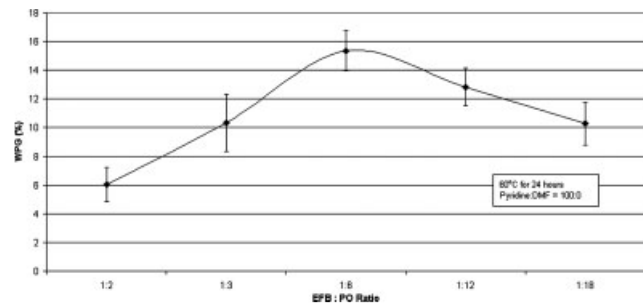


Figure 11 The effect of EFB : PO ratio on PO-modified EFB WPG (60°C, 24 h).

tilled water; W_3 , the weight (g) of density bottle filled with of toluene; W_4 , the weight (g) of density bottle with EFB (one-third full); W_5 is the weight (g) of density bottle with EFB and filled with of toluene.

Determination of hydroxyl content

To determine the OH content of EFB, ~ 3 g dried EFB (modified and unmodified) was weighted into a round-bottomed reaction flask. Twenty-five milliliter phthalating reagent (42.0 g of phthalic anhydride in 300 mL of dried pyridine) was added for esterification at 115°C for 3 h. Fifteen milliliter of pyridine was then added through the condenser to the cooled samples. The excess phthalic anhydride was then determined by titration with 0.5N NaOH to an end point of pH 9.2. The OH number, OH content, and equivalent weight of EFB can be calculated by using the following equations^{9,10}:

OH number

$$= \frac{56.1 \times N \text{ NaOH} \times (\text{mL blank} - \text{mL sample})}{\text{Sample weight (g)}}$$

$$\text{OH content (\%)} = \frac{\text{OH number}}{33}$$

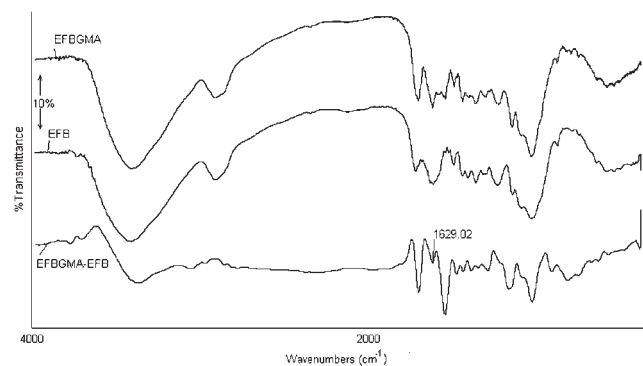


Figure 12 IR spectra of EFB-GMA, EFB and the subtraction of spectra.

TABLE I
Hydroxyl Content of EFB-GMA with Various WPG

Samples (WPG)	OH content (%)
EFB (0)	3.5 ± 0.3
EFB-GMA (9.76%)	4.8 ± 0.3
EFB-GMA (15.46%)	5.3 ± 0.2
EFB-GMA (21.41%)	5.2 ± 0.1
EFB-GMA (27.84%)	5.4 ± 0.2

$$\text{Equivalent weight of EFB} = \frac{56,100}{\text{OH number}}$$

The equivalent weight of unmodified EFB is 492 and this value is used in the chemical modifications of EFB.

Wide-angle X-ray diffraction (WAXD)

EFB (unmodified and modified) were ground into fine powder form. All the samples were dried before being analyzed using Siemens X-ray powder diffractometer model D5000 equipped with a CuK α target at 40 kV and 20 mA. Diffraction angle ranging from $2\theta = 0^\circ$ to 150° were recorded using a scintillation detector. The area under the peak was considered as the crystallinity of EFB (modified and unmodified).

Differential scanning calorimeter (DSC)

The predried EFB (unmodified and modified) were tested using Perkin-Elmer DSC6. Sample weight in the range of 10–15 mg was heated at $10^\circ\text{C}/\text{min}$ in the range of $30\text{--}440^\circ\text{C}$ with nitrogen atmosphere. For each sample, two measurements were made.

RESULTS AND DISCUSSION

Reaction condition

Figures 1 and 2 show the effects of solvent ratio (DMF : pyridine), reaction temperature, and reaction

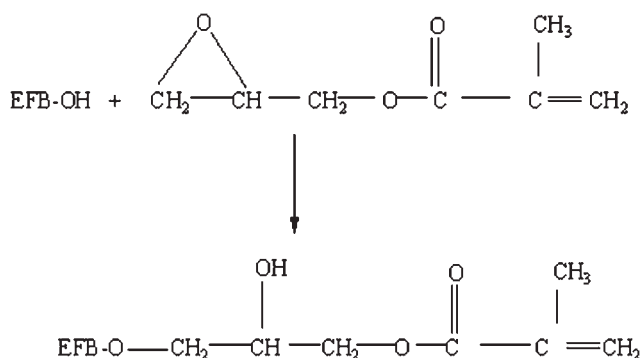


Figure 13 Reaction schematic of interaction between EFB and GMA.

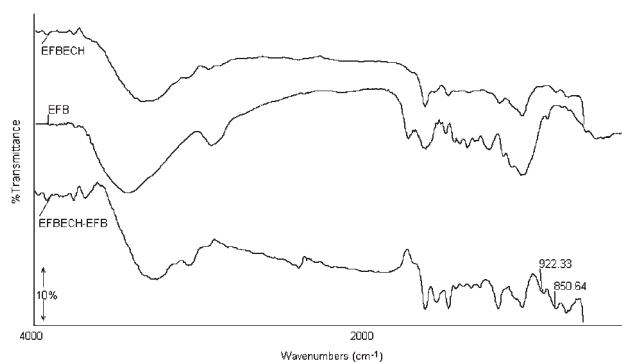


Figure 14 IR spectra of EFB-ECH, EFB and the subtraction spectra.

time on WPG of GMA-modified EFB (EFB-GMA). It is clearly shown that the WPG increases as the reaction temperature and reaction time are increased, but decreases with the increment in solvent ratio (DMF : pyridine). These findings are in agreement with Sun and Sun,¹¹ who reported that high temperature and long reaction time facilitate swelling of lignocellulosic materials and subsequently make the reactive site of lignocellulosic materials more accessible to reaction. It is important to note that the type and ratio of solvent have an influence on WPG. Pyridine is generally recognized as swelling agent cum catalyst. When pyridine alone is used, an uncontrollable exothermic reaction is triggered, which would degrade the EFB. According to Saunders,¹² polymerization of epoxy group could be catalyzed in the presence of amine, e.g., pyridine. However, this problem is not observed in DMF, which is an amide swelling agent that shows zero WPG when being used alone. Stamm⁷ reported that lignocellulosic materials showed higher swelling in DMF than in pyridine with the swelling index of 1.23 and 1.11, respectively. Thus, by taking consideration of these factors: (i) exothermic reaction and ability to catalyze the reaction of EFB and GMA by pyridine, (ii) swelling capability of DMF, the optimum condition for this GMA modification is fixed at 90°C for 3 h with solvent ratio of 50 : 50. EFB-GMA samples are prepared with different EFB:GMA (eq/eq) ratios at determined optimum condition. It is obvious that WPG increases with lower EFB:GMA ratio (Fig. 3). This is attributed to the amount of GMA that is increased with the reduction of the EFB:GMA ratio.

For ECH-modified EFB (EFB-ECH), the effects of solvent ratio, temperature, and time on WPG are

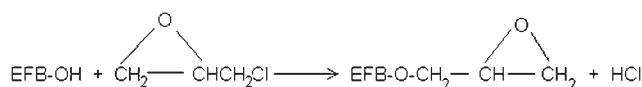


Figure 15 Reaction schematic of interaction between EFB and ECH.

TABLE II
Hydroxyl Content of EFB-ECH with Various WPG

Samples (WPG)	OH content (%)
EFB (0)	3.5 ± 0.3
EFB-ECH (7.21%)	1.3 ± 0.2
EFB-ECH (13.96%)	0.9 ± 0.3
EFB-ECH (22.49%)	1.1 ± 0.2
EFB-ECH (32.57%)	1.1 ± 0.2

shown in Figures 4–6. Based on the same justification made for EFB-GMA, the optimum condition is fixed at 90°C for 1 h with solvent ratio (DMF : pyridine) of 50 : 50. Subsequently, the EFB-ECH samples are prepared with different EFB/ECH ratios and it is found that the WPG increases as the EFB/ECH ratio is decreased (Fig. 7).

As for PO-modified EFB (EFB-PO), only pyridine is used as solvent because WPG drops drastically with the presence of DMF as cosolvent (Fig. 8). This shows that the reactivity of the EFB-PO reaction could only be activated if the pyridine is used alone as the solvent.

On the other hand, it is not surprising that only 15% WPG is achieved after 24 h reaction at 60°C (Figs. 9 and 10), which could be attributed to the low boiling point of PO (about 34°C). PO could be evaporated before it can interact with EFB. From the result obtained, it is suggested that the optimum condition for EFB-PO modification is 24 h at 60°C.

Figure 11 shows that WPG increases as the EFB:PO ratio is decreased to a level corresponding to 1 : 6, after which WPG decreases as the EFB : PO ratio is further reduced. This modification was carried out at determined optimum condition. The reduction observed could be attributed to reduction of pyridine while increasing the PO content to keep the volume constant. As a result, the evaporation point of the mixture (pyridine and PO) becomes lower. Hence, PO can be evaporated easily as compared to the mixture consists of lower content of PO.

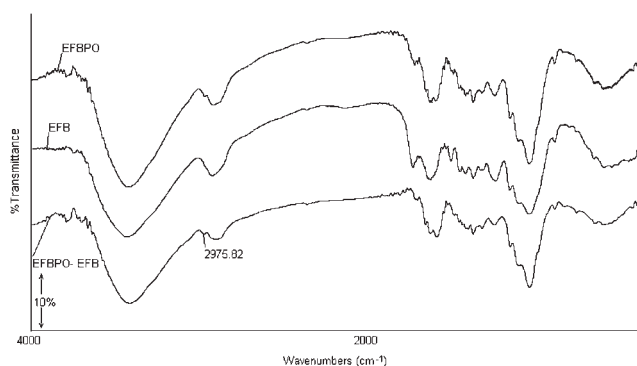


Figure 16 IR spectra of EFB-PO, EFB and the subtraction spectra.

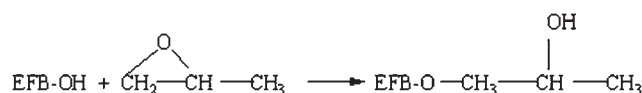


Figure 17 Reaction schematic of interaction between EFB and PO.

Rowell and Gutzmer¹³ reported that ECH showed the highest reactivity as compared to PO, butylene oxide and styrene oxide. This supports the results obtained in the present study where ECH shows the highest reactivity followed by GMA and PO.

Characterization

Figure 12 shows the IR spectra of EFB-GMA, EFB and their subtraction. The absorption at about 1630 cm^{-1} shows the evidence of C=C groups. Since the samples were extracted exhaustively with solvent to remove free reagent and homopolymer, this strongly indicates that GMA reacts with EFB and introduces C=C groups on the surface. This result is in line with the study carried out by Rozman et al.⁶ The increase in absorption in the C=C region at about 1630 cm^{-1} is due to the absorption of C=C of GMA. From the phthalation result (Table I), EFB-GMA shows an increment in OH content, which is about 5% as compared to untreated EFB (3.5%). The slight increase of OH content may be due to generation of new OH groups from the hidden OH groups in EFB, as a result of the reaction of GMA and EFB. The suggested chemical interaction between GMA and EFB is shown in Figure 13. These new OH groups would then interact with PU matrix during the preparation of PU composites. No significant difference is observed when the WPG is further increased.

The IR spectra of EFB-ECH, EFB, and the subtraction of these two spectra are shown in Figure 14. The absorption around 920 and 850 cm^{-1} are attributed to epoxy group and C-Cl linkages, respectively. It shows that ECH is chemically attached to the EFB though the reaction of epoxy group with OH of EFB (as depicted in Fig. 15). According to the study carried out by Rowell and Gutzmer,¹³ no loss of chlorine was observed in the reaction of wood with ECH. However, in this study, a fine powder material has been detected at the end of the reaction of EFB with ECH, which is probably due to the

TABLE III
Hydroxyl Content of EFB-PO with Various WPG

Samples (WPG)	OH content (%)
EFB (0)	3.5 ± 0.3
EFB-PO (6.08%)	7.8 ± 0.3
EFB-PO (10.53%)	7.8 ± 0.2
EFB-PO (15.36%)	8.1 ± 0.1

TABLE IV
Crystallinity of EFB Treated with GMA

Samples (WPG)	Crystallinity (%)
EFB (0)	29.45
EFB-GMA (9.76%)	34.58
EFB-GMA (27.84%)	28.17

formation of pyridine hydrochloride. The HCl formed in the reaction may have been eliminated through the formation of pyridine hydrochloride.¹⁴ This would avoid degradation of EFB from the acid attack. It is believed that pyridine hydrochloride has been removed by washing with acetone (under reflux condition) and also by mechanical sieving.

Hydroxyl (OH) content of the EFB-ECH samples is relatively lower as compared to the untreated EFB, which is about 3.5% (Table II). The OH content among EFB-ECH samples do not vary significantly as the WPG is increased. This observation indicates that OH groups from EFB have interacted with ECH through the epoxy group. Thus, this would reduce the hydrophilic nature of the EFB.

Figure 16 depicts the IR spectra of EFB-PO, EFB, and the subtraction of these two spectra. From the comparison of two spectra (EFB-PO and EFB), it is found that the small absorption around 2970 cm^{-1} and higher absorption around 3400 cm^{-1} are contributed by methyl (CH_3) and OH groups, respectively. This indicates that PO is chemically attached to EFB and could undergo further reaction in the presence of fresh PO, which would produce a polymer chain (Fig. 17). An increment of OH content is observed (Table III), which is about 8% with EFB-PO irrespective to the WPG. This observation is in agreement with Pavier and Gandini,¹⁵ which shows that higher OH number was observed with oxypropylated sugar beet pulp.

The crystallinity of EFB treated with GMA are shown in Table IV. For EFB with low level of modification, a small increase in the crystallinity of EFB is observed. According to a study carried out by Marcovich et al.¹⁶ and Canche-Escamilla et al.,¹⁷ this result evidently indicate that (i) the chemical reaction takes place in the amorphous region only because the chemical reagent cannot diffuse into the crystalline zone of the lignocellulosic materials; (ii) some of the constituents, for instance pectin, fat, wax, organic

TABLE V
Crystallinity of EFB Treated with ECH

Samples (WPG)	Crystallinity (%)
EFB (0)	29.45
EFB-ECH (7.21%)	34.26
EFB-ECH (32.57%)	26.67

TABLE VI
Crystallinity of EFB Treated with PO

Samples (WPG)	Crystallinity (%)
EFB (0)	29.45
EFB-PO (6.08%)	35.16
EFB-PO (15.36%)	34.84

acid, etc., have been removed when it is soaked in alkaline condition. This would result in an increase in crystallinity. This explanation is in line with the study carried out by Sydenstricker et al.¹⁸ According to Gassan and Bledzki¹⁹ the removal of other constituents would lead to better packing of cellulose chain. However, if the level of modification achieved to a certain extent, the crystalline region would be disrupted. According to Marcovich et al.,¹⁶ higher degree of grafting would give rise to more amorphous cellulose. This is resulted from the opening of hydrogen-bonded cellulose chain as the reaction proceeds, which would attribute to the decrease in crystallinity of lignocellulosic fiber. Shukla and Athalye²⁰ have attempted to study the characterization of GMA-grafted cellulose. They reported that at high WPG of GMA-grafted cotton sample, there was evidence of the disruption in crystallinity. This result is in line with the result obtained in the present study. It is clearly shown in Table IV that sample with a higher level of modification (about 28% WPG) exhibits lower crystallinity. A report by Mwaikambo and Ansell,² on the alkalization of lignocellulosic fiber found that the crystallinity of lignocellulosic fiber increased initially, but then decreased due to the cell wall damage when high concentration alkali was used. According to Rowell,²¹ the cell wall of lignocellulosic materials may be broken at about 30% WPG. Hence, the result obtained shows that GMA has interacted with the OH groups in the amorphous region of EFB. However, the crystalline region of EFB would be disrupted at high (about 30%) level of modification.

The effect of ECH modification on the crystallinity of EFB is shown in Table V. The results show a similar trend with GMA-modified EFB. Thus, the same explanation applies as in the previous discussion on GMA-modified EFB. On the other hand, Table VI indicates that the crystallinity of PO-modified EFB

TABLE VII
Density of GMA-Modified EFB

WPG (%)	Density (g/cm^3)
EFB (0)	1.31 ± 0.05
EFB-GMA (9.76)	0.95 ± 0.08
EFB-GMA (15.46)	0.96 ± 0.07
EFB-GMA (21.41)	0.97 ± 0.08
EFB-GMA (27.84)	1.03 ± 0.10

TABLE VIII
Density of ECH-Modified EFB

WPG (%)	Density (g/cm ³)
EFB (0)	1.31 ± 0.05
EFB-ECH (7.21)	1.22 ± 0.07
EFB-ECH (13.96)	1.21 ± 0.05
EFB-ECH (22.49)	1.19 ± 0.05
EFB-ECH (32.57)	1.19 ± 0.04

increases though there is no significant difference between samples with low and high WPG. This probably shows that at the highest WPG for PO modification, i.e., 15% WPG, the cell wall of EFB is still intact.

Tables VII–IX demonstrate the densities of treated and untreated EFB. In general, it can be seen that the density of treated EFB is lower than the untreated ones. This is in agreement with the investigation carried out by Sydenstricker et al.¹⁸ who studied sisal-reinforced polyester composite and reported chemical treatment would lead to a decrease in lignocellulosic fiber density due to the extraction of soluble elements in alkaline condition. Thus, the reduction of density on treated EFB is attributed to the formation of bigger dimension on treated EFB (swollen state) and some elements had been extracted from EFB during modification in alkaline condition. The density of EFB-GMA is relatively lower as compared to EFB-ECH and EFB-PO. This phenomenon could be explained with GMA, which has bigger molecule with seven-carbon atom, whereas ECH and PO contain three-carbon atom in the molecule. So, it is assumed that GMA would swell the EFB to a greater extent than does ECH and PO. Thus, the density of EFB-GMA is lower as compared to the others.

Figure 18 depicts the typical DSC thermograms for EFB, EFB-GMA (1 : 1), and EFB-GMA (1 : 4), respectively. It is obvious that an endotherm (150–200°C) is observed in the EFB DSC thermogram and this has shifted to a relatively higher temperature upon GMA modification. As shown in Table X, onset and peak temperature appear to increase with increasing the degree of modification. According to Tang and Eickner,²³ the endothermic peak observed in the range of 100–200°C may be attributed to the evapo-

TABLE IX
Density of PO-Modified EFB

WPG (%)	Density (g/cm ³)
EFB (0)	1.31 ± 0.05
EFB-PO (6.08)	1.22 ± 0.05
EFB-PO (10.53)	1.19 ± 0.04
EFB-PO (15.36)	1.18 ± 0.05

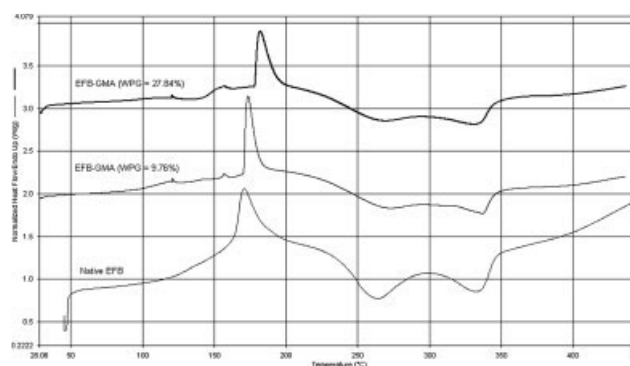


Figure 18 DSC thermogram of EFB and EFB-GMA.

ration of water and desorption of gases. At this stage, moisture contents in the EFB (treated and untreated), that could not be removed from the drying process at 105°C, may be evaporated. Bell and Eickner²⁴ reported that lignocellulosic materials degrade thermally in three distinct temperature range of pyrolysis, which are (i) moderately endothermic between 100 and 170°C, (ii) exothermic between 210 and 350°C, and (iii) decomposition above 350°C. So in the present context, it can be deduced that EFB-GMA experiences partial pyrolysis at relatively higher temperature as compared to the native EFB. In other words, EFB becomes more heat resistance upon GMA modification. However, the mechanism for the enhanced thermal degradation is not certain at this point. On the other hand, all DSC thermograms in Figure 18 show decomposition peaks between 250 and 400°C, which may correspond to splitting of cellulose macromolecule (259–389°C, exothermic), decomposition of hemicellulose (245–274°C), and decomposition of lignin (350–450°C, exothermic), respectively.²⁴ It is interesting to note that there are two small peaks appear in the DSC thermograms of EFB-GMA; the small exothermic peak in the range of 120–125°C, which is not observed in other treated EFB DSC thermograms. This could be resulted from the reaction of C=C groups from GMA that is detected from FTIR analysis in EFB-GMA. The double bond reacts with another C=C in vicinity. Hence, an additional linkage could be formed in this reaction; the small endothermic peak

TABLE X
Thermal Properties of EFB and EFB-GMA

EFB samples	Onset temperature (°C)	Peak temperature (°C)	ΔH (J/g)
EFB	165 ± 2	170 ± 2	38.1 ± 3.5
EFB-GMA (1 : 1)	171 ± 3	173 ± 4	38.5 ± 4.2
EFB-GMA (1 : 4)	178 ± 3	182 ± 3	37.4 ± 3.2

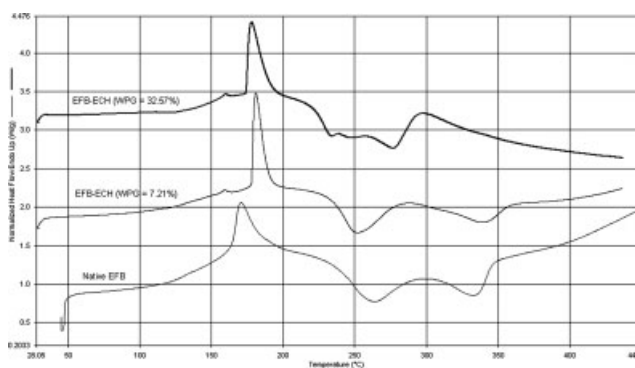


Figure 19 DSC thermogram of EFB and EFB-ECH.

around 150°C could be attributed to the presence of other traces of distinct crystallites formed from recrystallization of folded crystals, which occurs during the heating process.²⁵ However, this area would not be studied in detail.

In the case of EFB-ECH and EFB-PO (Figs. 19 and 20, Tables XI and XII), a similar trend shown by EFB-GMA is observed. In addition, EFB-ECH DSC thermogram shows a small exothermic peak at 200–250°C, which could be attributed to the reaction involving C–Cl chemically attached to the EFB. Beyond which, the subsequent thermal profile (250–400°C) of EFB-ECH with highest WPG is found to be distinctly differ from those of EFB and EFB-ECH with lower WPG. A plausible explanation to this observation could be the early decomposition of the lignocellulosic component (broken cell wall) as a result of a high degree (33%) of modification.²⁰

For EFB-PO sample, it can be seen that the peaks at 250–400°C (splitting of cellulose macromolecule and decomposition of hemicellulose) have been shifted to lower temperature as compared to the untreated EFB. This may be due to partial removal of hemicellulose when EFB is soaked in the alkaline condition for a long period (24 h).¹⁶

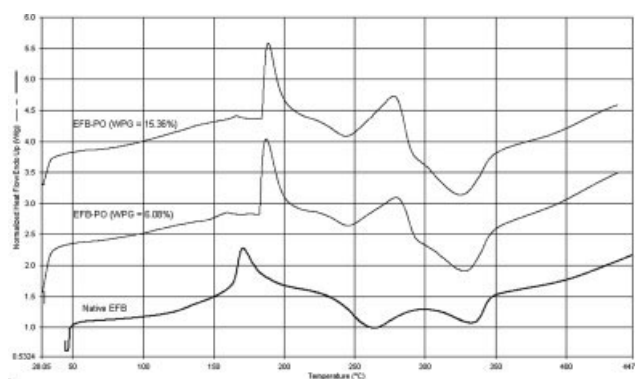


Figure 20 DSC thermogram of EFB and EFB-PO.

TABLE XI
Thermal Properties of EFB and EFB-ECH

EFB samples	Onset temperature (°C)	Peak temperature (°C)	ΔH (J/g)
EFB	165 ± 2	170 ± 2	38.1 ± 3.5
EFB-ECH (1 : 0.5)	178 ± 3	181 ± 2	38.6 ± 2.8
EFB-ECH (1 : 3)	174 ± 2	178 ± 2	39.3 ± 2.7

TABLE XII
Thermal Properties of EFB and EFB-PO

EFB samples	Onset temperature (°C)	Peak temperature (°C)	ΔH (J/g)
EFB	165 ± 2	170 ± 2	38.1 ± 3.5
EFB-PO (1 : 2)	189 ± 3	193 ± 2	38.0 ± 3.8
EFB-PO (1 : 6)	190 ± 4	193 ± 4	38.9 ± 2.6

CONCLUSIONS

Three types of chemical modification of EFB have been employed to modify the interfacial properties of the EFB-PU composites, i.e., GMA, ECH, and PO modification. In terms of reactivity of the reagent with EFB, ECH showed the highest followed by GMA and PO. FTIR analysis showed evidence that all reagents have chemically attached to the EFB with new or additional functional groups being generated. For EFB-ECH, epoxy groups have been regenerated; EFB-GMA, new OH groups have been generated from EFB hidden OH groups (5%) in addition to C=C groups, and EFB-PO with 5% additional of OH groups from EFB hidden OH groups and also methyl groups. The evidences that further reaction concerning these groups have occurred could be seen by the (i) polymerization of C=C with an exotherm at 120–125°C in the DSC thermogram of EFB-GMA, (ii) decomposition of C–Cl in EFB-ECH in the range of 200–250°C. The XRD scans showed that marginal increase in crystallinity was observed for EFB with low level of modification. This was attributed to the removal of alkaline extractable constituents from EFB. A disruption in EFB crystalline domain was obvious when WPG reached about 30%.

References

- Baiardo, M.; Frisoni, G.; Scandola, M.; Licciardello, A. *J Appl Polym Sci* 2002, 83, 38.
- Mwaikambo, L. Y.; Ansell, M. P. *J Appl Polym Sci* 2002, 84, 2222.
- Santayanon, R.; Wootthikanokkhan J. *Carbohydr Polym* 2003, 51, 17.

4. Rowell, R. M. In *Science and Technology of Polymer and Advanced Materials: Emerging Technologies and Business Opportunities*; Prasad, P. N.; Mark, J. E.; Kandil, S. H.; Kafafi, Z. H., Eds.; Plenum Press: New York, London 1998; p. 717-732.
5. Tay, G. S. M.Sc. Thesis Universiti Sains Malaysia, 2002.
6. Rozman, H. D.; Musa, L.; Abubakar, A. *J Appl Polym Sci* 2005, 97, 1237.
7. Stamm, A. J. *Wood and Cellulose Science*. The Ronald Press, 1964.
8. Lewis, M. J. *Physical Properties of Foods and Food Processing and Food Processing Systems*; Ellis Horwood: New York, 1990.
9. David, D. J.; Staley, H. B. *High Polymers Series: Analytical Chemistry of the Polyurethanes, Part III*; Interscience: New York, 1969; Vol. XVI.
10. Doyle, E. N. *The Development and Use of Polyurethanes Products*; McGraw-Hill: New York, 1971.
11. Sun, R. C.; Sun, X. F. *Indust Crops Products* 2002, 16, 225.
12. Saunders, K. J. *Organic Polymer Chemistry*; Chapman and Hall: London, 1988.
13. Rowell, R. M.; Gutzmer, D. I. *Wood Sci* 1975, 9, 240.
14. Pacansky, T. J.; Schank, R. L.; Gruber, R. J.; Brandt, K. A.; Bernad, M. *J Polym Sci: Polym Chem Ed* 1980, 18, 3119.
15. Pavier, C.; Gandini, A. *Indust Crops Products* 2000, 12, 1.
16. Marcovich, N. E.; Aranguren, M. I.; Reboredo, M. M. *Polymer* 2001, 42, 815.
17. Canche-Escamilla, G.; Cauich-Cupul, J. I.; Mendizabal, E.; Puig, J. E.; Vazquez-Torres, H.; Herrera-Franco, P. J. *Compos A: Appl Sci Manufact* 1999, 30, 349.
18. Sydenstricker, T. H. D.; Mochnaz, S.; Amico, S. C. *Polym Testing* 2003, 22, 375.
19. Gassan, J.; Bledzki, A. K. *J Appl Polym Sci* 1999, 71, 623.
20. Shukla, S. R.; Athalye, A. R. *J Appl Polym Sci* 1995, 57, 983.
21. Rowell, R. M. *Forest Products Abstracts* 1983, 6, 363.
22. Chen, R. H.; Tsaih, M. L.; Lin, W. C. *Carbohydr Polym* 1996, 31, 141.
23. Tang, W. K.; Eickner, H. W. U.S. Forest Service Research Paper, FPL 82 1968.
24. Beall, F. C.; Eickner, H. W. U.S.D.A. Forest Service Research Paper, FPL 130 1970.
25. Bershtein, V. A.; Egorov, V. M. *Differential Scanning Calorimetry of Polymer: Physics, Chemistry, Analysis, Technology*; Ellis Horwood: New York, 1994.